Process Safety and Environmental Protection 121 (2019) 103–117

Contents lists available at ScienceDirect

Process Safety and Environmental Protection

journal homepage: www.elsevier.com/locate/psep

A comparative optimization and performance analysis of four different electrocoagulation-flotation processes for humic acid removal from aqueous solutions

Gona Hasani[a], Afshin Maleki[b,*], Hiua Daraei[b], Reza Ghanbari[c], Mahdi Safari[b], Gordon McKay[d,*], Kaan Yetilmezsoy[e,*], Fatih Ilhan[e], Nader Marzban[f]

[a] Student Research Committee, Kurdistan University of Medical Sciences, Sanandaj, Iran
[b] Environmental Health Research Center, Research Institute for Health Development, Kurdistan University of Medical Sciences, Sanandaj, Iran
[c] Social Determinants of Health Research Center, Qazvin University of Medical Sciences, Qazvin, Iran
[d] Division of Sustainability Development WR JHM CEJ, College of Science and Engineering, Hamad Bin Khalifa University, Education City, Qatar Foundation, Doha, Qatar
[e] Department of Environmental Engineering, Faculty of Civil Engineering, Yildiz Technical University, Davutpasa Campus, 34220, Esenler, Istanbul, Turkey
[f] ACECR Institute of Higher Education, Isfahan Branch, Isfahan, Iran

ARTICLE INFO

Article history:
Received 31 July 2018
Received in revised form 9 September 2018
Accepted 24 October 2018
Available online 26 October 2018

Keywords:
Alternating pulse current
Electrocoagulation-flotation
Electrode morphology
Humic acid
Design of experiments
Taguchi method

ABSTRACT

Humic substances (HSs) are a group of complex macromolecular polymeric compounds originating from the decomposition of plant residuals and other organic matter. Within the presence of micro-pollutants and heavy metals, HSs negatively act upon potable water quality by contributing to aesthetic problems such as yellowish or brownish color and annoying taste and odor. They are also responsible for re-growth of pathogenic microorganisms and fouling of membranes in water distribution systems. More importantly, these high-molecular-weight polymers have been noted to be the major contributor to the formation of disinfection by-products (DBPs) such as trihalomethanes (THMs) and haloacetic acids (HAAs). Considering these harmful effects, removal of HSs is one of the significant tasks in drinking water treatment. For this purpose, this study aimed to explore the effects of various operating parameters (initial concentration, initial pH, electrical conductivity, pulse time, pulse number, and process time) on the humic acid (HA) removal efficiency and energy consumption. In this study, a new current supply method called alternating pulse current electrocoagulation-flotation (APC-ECF) process was proposed, and a detailed comparative optimization of four different ECF processes (direct current (DC)-simple electrode, DC-perforated electrode, pulse current-simple electrode, and pulse current-perforated electrode) was conducted within the framework of Taguchi-based experimental design methodology. According to scanning electron microscopy (SEM), the morphology of electrode surfaces with APC and perforated electrode showed less disordered (irregular) pores and a regular structure of aluminum compared to the DC, which confirmed the difference in the corrosion rates. Moreover, the proposed APC-ECF method led to the production of less dewatered and dense sludge. The results of the performance analysis revealed that the APC with a perforated electrode provided 3.2-fold lower energy consumption and 2.5-fold lower aluminum consumption compared to the DC with a simple electrode. Considering the expenses associated with power consumption and sludge disposal costs for the electrocoagulation unit, the experimental findings corroborated that the proposed APC-ECF process could be used as a promising and cost-effective technology in water treatment for the removal of HSs.

1. Introduction

Contamination of drinking water is one of the worldwide problems that is of great concern as it imposes a severe threat on biotic life. Introduction of contaminants into the water environment through various pathways causes deleterious effects on humans and other living organisms, thus deteriorating the quality of life irreversibly in some cases (Bajpai et al., 2014; Sani et al., 2017).

* Corresponding authors.
E-mail addresses: gona.hasani@muk.ac.ir (G. Hasani), malaki@muk.ac.ir (A. Maleki), hiua.daraei@muk.ac.ir (H. Daraei), r.ghanbari@qums.ac.ir (R. Ghanbari), safari.m@muk.ac.ir (M. Safari), gmckay@hbku.edu.qa (G. McKay), yetilmez@yildiz.edu.tr (K. Yetilmezsoy), filhan@yildiz.edu.tr (F. Ilhan), n.marzban@ce.iut.ac.ir (N. Marzban).

https://doi.org/10.1016/j.psep.2018.10.025
0957-5820/

Among various types of pollutants, the presence of natural organic matter (NOM) in drinking water causes many problems in the water treatment processes. Humic substances (HSs) are considered as the most abundant NOM and originate from microbial activity and decomposition of plant and animal remnants in nature (Eish and Wells, 2006). The HSs constitute 60–90% of NOM (Sachse et al., 2005), and they are among major concerns in drinking water treatment. A combination of these substances with heavy metals (Alswat et al., 2017a,b), which are mostly carcinogenic, facilitates their transfer to water resources, and the presence of these substances in treated water causes re-growth of pathogenic microorganisms in water distribution networks (Crittenden et al., 2005; Maleki et al., 2016a). Furthermore, these substances lead to fouling of membrane filters (Saleh, 2015a,b; Saleh, 2016) and anionic resins and prevent oxidation of iron and manganese (De la Rubia et al., 2006; Maleki et al., 2016b; Wang et al., 2018). However, the most important problem caused by such substances is their contribution as a precursor to the production of disinfection by-products (DBP). For this reason, more disinfectant is used in the process, so that the risk of the formation of DBP increases despite increased disinfection efficiency. Trihalomethanes (THMs) are among the most important by-products of chlorine disinfection (Kawamura, 2000; Mahvi et al., 2009). They have no specific smell in water but are physiologically associated with health hazards such as gene mutation and cancer (Li et al., 2011; Maleki et al., 2016b).

The United States Environmental Protection Agency (US EPA) has set a maximum concentration level (MCL) of 80 ppb for total THMs and 60 ppb for five haloacetic acids (HAA5) (Rodriguez et al., 2004). Nevertheless, the United Kingdom (UK) standard for trihalomethanes is 100 μg/L, while the trihalomethane formation potential for natural organic substances is above 100 μg/mg of dissolved organic carbon (DOC). Therefore, nearly 1 mg/L of the residual DOC can violate the previous standard (Murray and Parsons, 2006). Considering the current strict rules and the harmful effects of HSs, they must be removed from drinking water.

So far, several methods, including coagulation (Wang et al., 2012; Yu et al., 2013), adsorption (Rauthula and Srivastava, 2011), Fenton reactions (Wei et al., 2011), nano-photocatalysts (Maleki et al., 2016a), photocatalytic membranes (Rao et al., 2016; Szymański et al., 2016), membrane filtration (Jafari et al., 2015), biological treatment (Moura et al., 2007), and ozonation (Seredynska-Sobecka et al., 2006), have been conducted for humic acid (HA) removal from drinking water. Recently, in developed countries, electrochemical techniques have been successfully applied to various environmental issues (Holt et al., 2002; Feng et al., 2007; Yetilmezsoy et al., 2009a; Safari et al., 2014). The electrocoagulation-flotation (ECF) process with direct current (DC) includes the production of coagulant through electrical dissolution of a sacrificial anode. These coagulants (such as aluminum hydroxide), due to their large surface area, quickly adsorb soluble organic compounds and entrap the colloidal particles. Agglomerate clots are formed, precipitated, or floated through flotation by hydrogen gas produced at the cathode that appears in the form of small bubbles (Wang et al., 2009). However, in electrocoagulation with DC, after a certain time, an impermeable oxide layer is formed on the cathode. This prevents effective transmission of current within the system, leading to higher power costs and lower efficiency. This problem is intensified with an aluminum electrode. In general, the increased consumption of the electrode and electrical energy and increased production of sludge are among the major disadvantages of this method. Typically, power consumption costs account for more than 50% of electrocoagulation unit expense (Mollah et al., 2001). Therefore, improvement of the electrode processes used in electrocoagulation is highly necessary. Although the previous electrochemical-based treatability studies have made important contributions to this area, the plurality of them only addresses the effect of the existent process conditions on the removal of a specific contaminant from different wastewaters. To the best of the authors' knowledge, there is still an apparent gap in the relevant field concerning the investigation of novel and cost-effective ECF installations to alleviate the above-mentioned disadvantages associated with power consumption and sludge disposal. It seems from the literature that there are almost no systematic papers specifically devoted to a study of a comparative optimization of different ECF combinations for HA removal from aqueous solutions within the framework of Taguchi-based experimental design methodology. In this context, the present study was introduced as a new attempt to fulfil the mentioned gap by focusing upon a detailed quantitative performance analysis of four ECF processes (DC-simple electrode, DC-perforated electrode, pulse current-simple electrode, and pulse current-perforated electrode) within the experimental domain of the various operating factors.

In consideration of the foregoing facts, in the present study, a novel current supply method called alternating pulse current electrocoagulation-flotation (APC-ECF) was proposed to overcome the disadvantages of electrocoagulation with DC. This current can be applied using an alternating pulse circuit at the DC source's output to convert the DC into a pulse, alternating current. Using this current supply model at certain time intervals, the current direction, and consequently, the electrodes' role is changed. Such switching on and off of the current (pulsating) and change in the electrode role (alternating) not only prevent passivation of the cathode electrode, but also provide sufficient time for the coagulants to complete the coagulation reaction due to the off-time between each pulse, which in turn leads to reduced energy consumption (Mao et al., 2008). The current is used with square, sinusoidal, and triangular waveforms in pulsed electrolysis; however, pulsed currents with square wave forms (symmetrically and asymmetrically) are more widely used in electrolysis (Sahay and Kushwaha, 2017).

2. Materials and methods

2.1. Preparation of stock solution

The HA used in the present study was purchased from the Sigma Aldrich Corporation, and the 98% perchloric acid and sodium hydroxide for pH adjustment as well as nitrate-potassium salt for providing the required electrical conductivity, were purchased from the Merck Corporation. The present study was conducted in a 1-L glass reactor with discontinuous current. To prepare the 1 g/L stock HA solution, 1 g of HA was completely dissolved in 62.5 mL of 2 N NaOH. After complete dissolution, it was diluted to a volume of 1 L using distilled water (with conductivity of 10 μS/cm at 25 °C). Then, it was placed on a magnetic stirrer for 48 h. The prepared stock solution was stored at 4 °C away from light. The synthetic samples were made from stock HA solution, and their pH was adjusted by adding sufficient amounts of appropriate base and acid.

2.2. Equipment used in the experimental tests

The devices used in this study included an electricity generator (RXN-303D Model) manufactured by ZHAOXIN Corporation, a spectrophotometer (T80 Model), a pH meter and a conductivity meter (Jenway Model) made in England, a KN-70 centrifuge manufactured by KUBOTA Co., Japan, a voltmeter & ampere-meter (DT830D Model) manufactured by GILSUN Co., China, a scanning electron microscope (MIRA3 model) manufactured by T-Scan Co., Czech, Atoc meter (SKALAR Model) made in the Netherlands, and a hand-made pulse device.

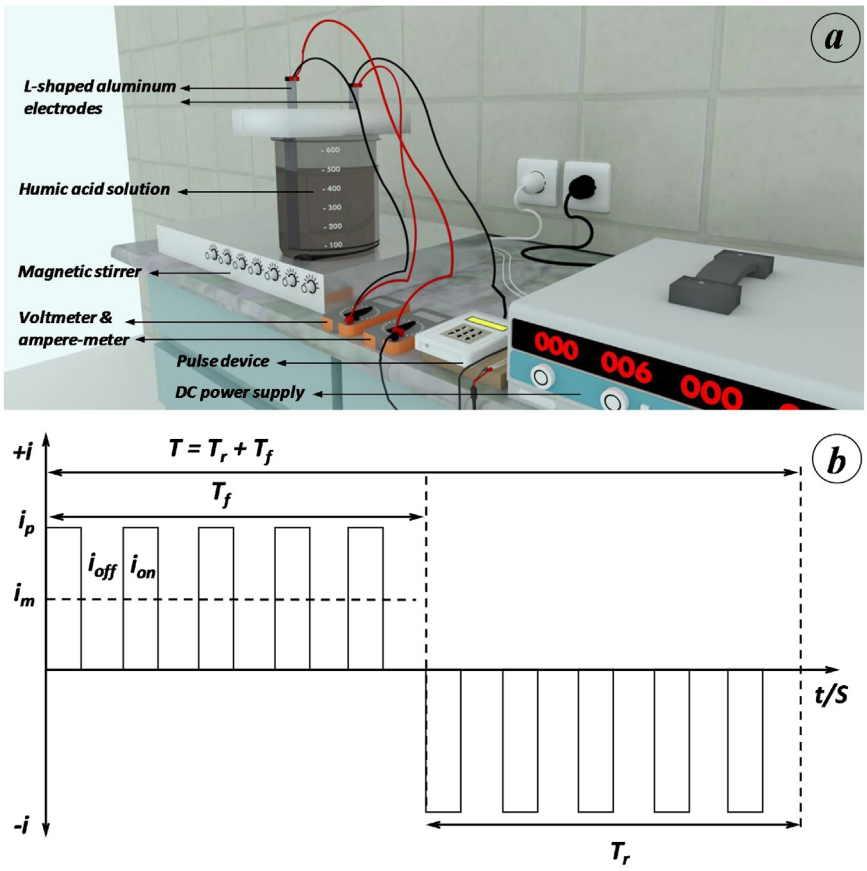

Fig. 1. (a) Reactor used in electrocoagulation-flotation with alternating pulse current; and (b) shape of pulses in applied alternating pulse current.

2.3. Experimental set-up and procedure

Two L-shaped aluminum electrodes were embedded in the reactor in unipolar mode with an effective surface area of 100 cm^2 at 1 cm distance from each other, and 20 pores with a diameter of 4 mm were created on the surface of each electrode. The electrodes were connected to the pulser, which was connected to a DC electric generator. The generated DC entered the pulser, and the pulser output current was transmitted to the electrodes. The coagulation process mixture was provided using a magnetic stirrer with mixing speed of 50 rpm (≈ 10.47 rad/s). During the process, the potential difference applied to the electrodes and the generated currents were measured using a voltmeter and ampere-meter, respectively (to ensure establishment of current and execution of the process).

Fig. 1a illustrates the reactor used in the electrocoagulation-flocculation process with APC. Fig. 1b shows the shape of the pulses created by the pulser in this study with a pulse number variable of 5. As seen in this schematic, after applying every five square-shaped pulses the electrode positions were changed by changing the current direction. In this diagram, T_f is the cycle's positive period, T_r is the cycle's negative period, t_{on} and t_{off} indicate the times when the current in the circuit is ON and OFF, respectively, T indicates the total time of a current cycle, i_p is the current density peak at T_f, and i_m represents the average density.

2.4. Taguchi-based experimental design methodology

For a multivariable environmental process, investigation of the main and the interaction effects of various process-related parameters on the response is an important task to gain a better understanding of the operative mechanism of the studied system. However, determination of all possible combinations of the test variables is impractical and time-consuming since a large number of experiments is required to implement this task (Yetilmezsoy et al., 2009b). For this reason, implementation of a systematic experimentation methodology to minimize the number of tests while evaluating the effects of important parameters along with possible interactions can be a cost-effective and strategic approach (Yetilmezsoy et al., 2009b; Hasani et al., 2018). At this point, experimental design or design of experiments (DOE) methodology makes it feasible to observe the possible interaction of the parameters and their influences on the response variable in a cost- and time-effective way (Saleh et al., 2017).

The Taguchi method is a standardized version of DOE that is used to determine the effect of factors on the response and optimal conditions for the systems (Daneshvar et al., 2007). The prime motivation behind the Taguchi-based experimental design (Taguchi/DOE) technique is the reduction of variations around the target without actually removing the cause of variation. Another motive why Taguchi/DOE method provides a consistent analysis over classical DOE is the advantage of attaining robustness in the functional performance by inducing the existence of noise factors (i.e. factors that are not controllable or are too expensive to control) during the experiment. In this robust design strategy, a logarithmic transformation of mean squared deviation (MSD), which is referred as the signal-to-noise (S/N) ratio, is used for the analysis of results. In other words, in the Taguchi methodology, for more precise statistical analysis of the obtained results, a converted response function is used, which is defined as the ratio of sign of each effect (S) to the effects of each error (N). The advantage of using this new response in statistical analysis, compared to the primary form of the response, is the capability of comparing the magnitude of the

effects from each major factor to effects from turbulence and error factors in measurement. This will consequently lead to a more accurate understanding of the actual effect of factors on the system. In Taguchi/DOE approach, the S/N ratio is calculated for each factor level combination depending on the goal (i.e. smaller is better, larger is better, nominal is best) of the conducted experiment. In all cases, the S/N ratio is maximized to minimizes the effect of noise on the response, so that the experimental condition having the maximum S/N ratio is considered as the optimal condition (Oztop et al., 2007; Daneshvar et al., 2007; El khalidi et al., 2018).

Considering the foregoing facts, in the present study, the effect of the effective operating parameters of the process on removal efficiency of HA was investigated within the framework of the DOE methodology using Taguchi approach. Since the HA removal rate was considered the present response, the objective was to maximize this output. Considering this global idea, "larger is better" type of optimization was used to maximize the S/N ratio (El khalidi et al., 2018):

$$S/N = -10\log\left[\frac{1}{n}\sum_{i=1}^{n}\left(\frac{1}{Y_i}\right)^2\right] \quad (1)$$

where n is the number of the repeated experiments, and Y_i is the measured experimental value.

2.5. Analytical procedure and calculations

In each experiment, 500 mL of the synthetic HA sample was used at room temperature under the operational conditions mentioned in Table S2. In each experiment at 10, 20, 30, 50, and 70 min, 40 cc of sample was transferred to glass vials, and the samples were centrifuged at 3000 rpm (≈ 314.16 rad/s) for 10 min. The sample overflow was removed by pipette, and after transmission to a 4-cc quartz cell, the sample's adsorption rate was read by the spectrophotometer at 254 nm. Using the calibration curve, the adsorption signal was converted to concentration (mg). In the next phase, the removal efficiency was calculated using Eq. (2). For each sample, the final pH and EC were measured. The zero samples were taken from the reactor before initiating the process.

$$R = \frac{C_0 - C_e}{C_0} \times 100 \quad (2)$$

where C_0 and C_e indicate initial and final concentrations of HA (mg/L), respectively, and R is the removal efficiency (%). Afterwards, removed HA mass (mg) was calculated in Eq. (3) using the calculated efficiency, the initial concentration, and reactor volume:

$$m_{HA(mg)} = \frac{R}{100} \cdot C_0 \cdot V_r \quad (3)$$

where m_{HA} is removed HA mass (mg) and V_r is the reactor volume (0.5 L). Additionally, the produced aluminum mass and energy consumption rate were determined, respectively, using Eqs. (4) and (5) as follows (Martinez-Huitle and Brillas, 2009; Wang et al., 2009; Mohora et al., 2014; Alimohammadi et al., 2017):

$$m_{Al} = (M \cdot I \cdot t_p)/(z \cdot F) \quad (4)$$

$$E = (U \cdot I \cdot t)/V_w \quad (5)$$

where m_{Al} is the released aluminum's mass (g), I is the current intensity (A), t_p is the process time or duration of operating time (s), F is the Faraday's constant (96,485 C/mol, where 1 Faraday = 96,485 coulombs (C), and 1 C = 1 A × 1 s), M is the molecular weight of aluminum (0.02698 kg/mol for Al), z is the number of electrons involved in the oxidation/reduction reaction (z = 3 for Al), E is the energy consumption rate or specific electrical energy consumption of the process (kWh/m^3, where 1 W = 1 A × 1 V), U is the potential difference (V), t is the time (h), and V_w is the volume of treated water (m^3).

Table 1
Regression coefficients estimated by multiple linear regression model.

Term	Regression coefficient	*p*-value[a]
Constant	−2.937	0.015
C_0 (mg/L)	0.436	0.000
EC_0 (μS/cm)	−0.002	0.000
pH_0	0.366	0.000
T_{pls} (min)	0.172	0.001
t (min)	0.021	0.023

[a] *p* values < α = 0.05 are significant.

Table 2
Analysis of variance (ANOVA) for assessing the effect of categorical factors on the response and testing the significance of the HA removal model for the APC-ECF process.

Source	*df*	Seq SS	Adj SS	Adj MS	*F*-value	*p*-value
Regression	5	7156.77	7156.77	1431.35	284.41	0.000
Linear	5	7156.77	7156.77	1431.35	284.41	0.000
C_0 (mg/L)	1	6801.89	6964.40	6964.40	1383.84	0.000
EC_0 (μS/cm)	1	164.23	140.55	140.55	27.93	0.000
pH_0	1	110.07	109.38	109.38	21.73	0.000
T_{pls} (min)	1	53.81	53.25	53.25	10.58	0.001
t (min)	1	26.78	26.78	26.78	5.32	0.023
Residual error	127	639.15	639.15	5.03		
Total	132	7795.92				

df = Degrees of freedom; Seq SS = Sequential sums of squares; Adj SS = Adjusted sums of squares; Adj MS = Adjusted mean squares; *F*-value is the test statistic used to determine whether the term is associated with the response; *p*-value is a probability that measures the evidence against the null hypothesis; R^2 = 0.918; and *p* values < 0.05 are significant.

3. Results and discussion

3.1. Model development and statistical results

A total of 27 experiments were performed to investigate the operational conditions, and the results of which are schematically presented in Fig. 2. The effect of different operational conditions is evident in the experiments. According to the experimental results, the removal efficiency was 6–100%. Statistical investigation of the operational parameters was performed via several statistical analyses on the collected data. For this purpose, multiple linear regression based on the analysis of variance (ANOVA) was used to determine the effective parameters and test the significance of the obtained HA removal model for the experimental data. ANOVA can estimate the influence of a factor on the characteristic properties, and experiment can be conducted with the minimum replication using the orthogonal arrays (Oztop et al., 2007). The results of the statistical analyses (for a confidence level of 95%) are presented in Tables 1 and 2.

According to Table 1, among the studied operational parameters, the variables of initial concentration, electrical conductivity, pH, pulse time, and process time were significant at α = 0.05, which indicated the great importance of these factors for HA removal rate. Eq. (5) shows that initial concentration, pH_0, pulse time, and process time have a positive effect on the process, and EC_0 negatively affects the HA removal. The model obtained from this method is presented in Eq. (6). The value of R^2 is equal to 0.918, and the coefficient of determination ranges between 0 and 1, indicating that it is an acceptable linear empirical model.

$$HA\ removal(\%) = -2.937 + 0.436(C_0) - 0.002(EC_0) + 0.366(pH_0) + 0.172(T_{pls}) + 0.021(t) \quad (6)$$

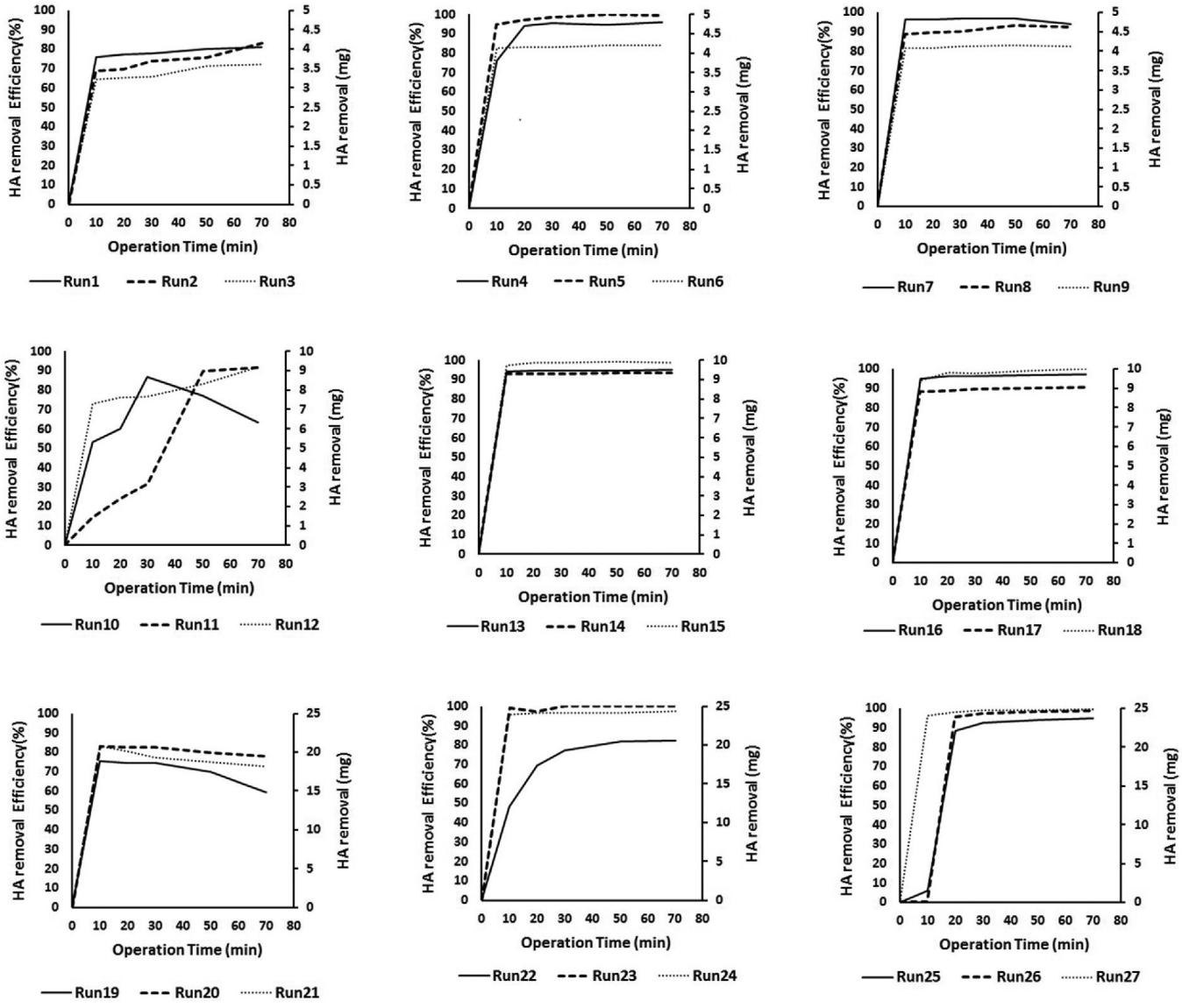

Fig. 2. Variation of HA removal efficiency with operation time in 27 different runs (C_0 = 10–50 mg/L, pH_0 = 3–9, EC_0 = 500–2000 μS/cm, T_{pls} = 1–10 min, N_{pls} = 1–10, and V = 5–15 V).

3.2. Taguchi orthogonal experimental design methodology

Within the framework of the implemented Taguchi/DOE methodology, the first step was to select the effective process-related operating parameters. For this purpose, the variables including initial HA concentration, electrical conductivity, pH, voltage, pulse time, and number of pulses were chosen for optimization. Then, each variable was investigated at three levels (low, center, and high) in accordance with Table S1. Considering the number of factors and their respective levels, the L27 orthogonal array of the Taguchi method was used to determine interactions between experimental factors. Table S2 presents the Taguchi/DOE matrix for the levels of each variable specified in this study. This matrix [27×6] contains three-levels for six independent variables selected for optimization and performance analysis of different electrocoagulation-flotation processes. Finally, data analysis was performed using Minitab 16 software (Minitab Inc., State College, PA).

According to Fig. 3a and b, the optimal values for response optimization were determined as 50 mg/L for initial concentration, 7 for initial pH, 10 min for pulse time, 500 μS/cm for electrical conductivity, and 70 min for operation time. Furthermore, the rating of each parameter in the response rate was as follows: Concentration (C_0) > pH_0 > process time (t) > pulse time (T_{pls}) > electrical conductivity (EC_0).

3.3. Parameters affecting HA removal

3.3.1. Effect of initial pH

pH is an important factor in electrical coagulation processes that can influence the process efficiency in two ways. First, by affecting the distribution of aluminum hydrolysis products, it can influence process efficiency. According to the colorimetric analysis and nuclear magnetic resonance (NMR) of Al, different types of aluminum, namely, Al_a, Al_b, and Al_c include monomeric species ($Al(OH)^{2+}$, $Al_2(OH)_2{}^{4+}$, $Al_3(OH)_4{}^{5+}$), medium polymers ($AlO_4Al_{12}(OH)_{24}(H_2O)_{12}{}^{7+}$, Al_{13}), and colloidal and solid types ($Al(OH)_3$), respectively. The Al_b species are known as Al_{13} polymer. Having high positive charge and powerful bonding ability, Al_{13} polymer is the most active species responsible for coagulation. The hydroxyl ion produced at the cathode surface causes formation of Al(OH)−4; in addition, OH−, which is continuously produced at the

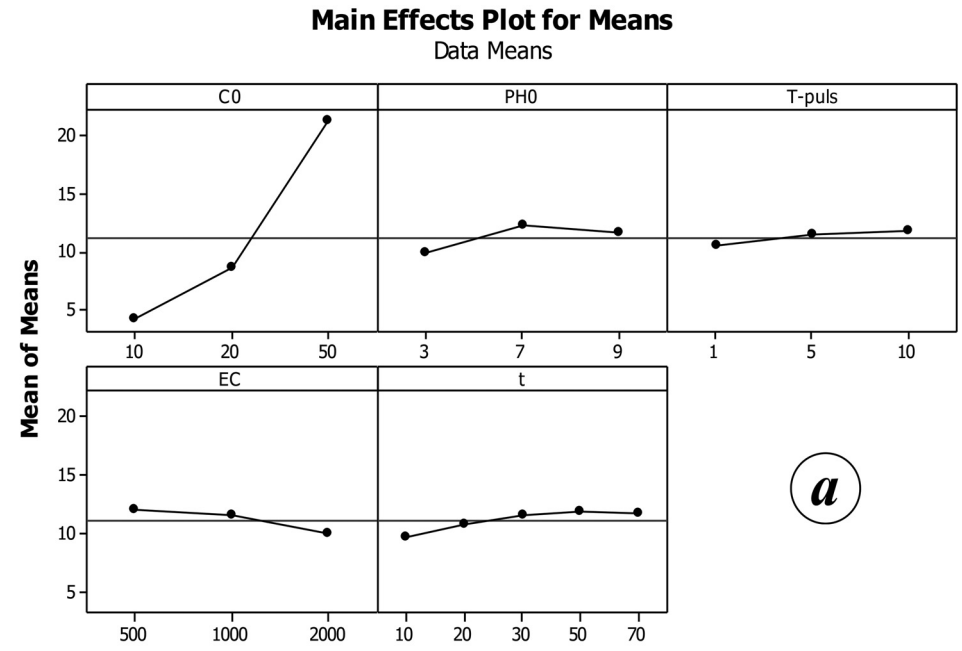

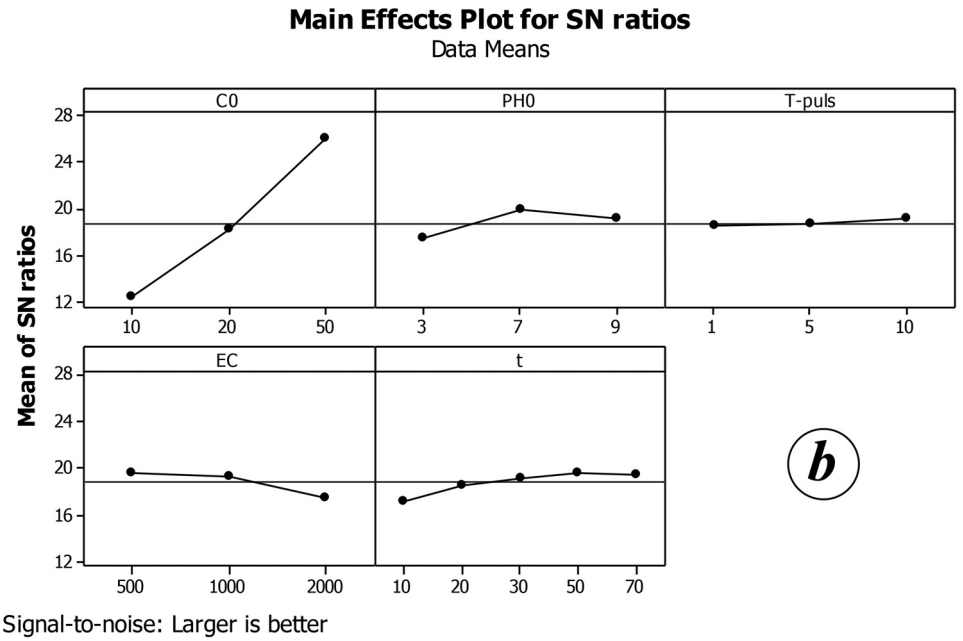

Fig. 3. (a) Diagram for effects of average data values in Taguchi/DOE analysis, and (b) diagram for S/N in Taguchi analysis for the optimal values of C_0 = 50 mg/L, pH_0 = 7, T_{pls} = 10 min, EC_0 = 500 μS/cm, and t = 70 min.

cathode, causes formation of an area with high pH that induces formation of Al(OH)$_{-4}$. Al(OH)$_{-4}$ reacts with monomers and dimers to form Al_{13}, which is a mediator in the production of $Al(OH)_3$ deposits (Fig. S1) (Hu et al., 2016).

According to Fig. 1, the removal of HA occurred mostly in the first 10 min. In addition, according to the diagram in Fig. S2 presented by Hu et al. (2016), in the first 10 min, $Al_b(Al_{13})$ was the most prevalent species. Therefore, it can be concluded that the Al_b is the main species responsible for coagulation. This large polymer, with high surface charge, has a great potential for neutralizing the negative charge of HA. Furthermore, not only via neutralization but also due to its large surface, it causes adsorption and splicing (bridging) between particles. Subsequently, as hydrolysis time increases, due to the higher production rate of hydroxyl ions in the cathode, the pH of the environment gradually reaches to 8–9, leading to precipitative formation of $Al(OH)_3$. Therefore, after the 10th min, the removal percentage can be seen with a slight slope, due to the entrapment of the particles between hydroxide deposits and the sweeping mechanism.

Due to the use of APC in the present study, the role of electrodes was alternatively changed, and thus no concentration gradient causing any accumulation of HA on the anode was formed, so that adverse process conditions were alleviated without any operational problem. For the present case, highest efficiency was observed at pH of 7. On the other hand, the relatively lower efficiency obtained at pH 9 can be attributed to the reduced zeta potential and increased negative charge of HA. This phenomenon occurs because of the loss of protons in some of the functional groups of HA (Gregor et al.,

1997; Lu et al., 1999). As a result of the increased negative charge at high pH values, the system requires more aluminum to complete the bonding capacity of humic substances, which is another reason for the reduced removal efficiency (Koparal et al., 2008).

As a result of the electrochemical process, the reaction pH increased due to the production of hydroxyl ions in the aqueous solution. At the initial pH of 3, despite a moderate increase of 2 units, the system efficiency was low since pH was still in the acidic range. When the initial pH of the reaction was neutral, the pH of the reaction increased, and the final pH of reaction eventually reached 8.7. Finally, when the initial pH of reaction was 9, pH was slightly increased, and the final pH reached 9.47. Therefore, during the reaction at pH 7–9, the reaction was eventually alkalinized, and the reactions occurred at an alkaline pH. Accordingly, some slight changes occurred in the removal efficiency at this pH range.

Studies conducted by Bazrafshan et al. (2007), Malakootian et al. (2011), and Zaleschi et al. (2014) indicated that electrocoagulation serves as a pH adjustor, consistent with the present study. Based on the results obtained in this section, it can be inferred that since electrocoagulation itself serves as a buffer, using this process in water and wastewater treatment plants does not require pH adjustment at the beginning of the process; however, at the end of the process, pH might need to be adjusted due to the increased output pH in some operational conditions.

3.3.2. Effect of process time (t)

According to Faraday's law, the electrolysis time in electrocoagulation processes affects the production of metal ions. At the beginning of the process, the removal efficiency of HA versus time is increased with a steep slope, so that the highest HA removal rate in experiments shown in Fig. 1 occurs at 10 min; subsequently, the removal efficiency increases with a slight slope. Therefore, the removal process can be divided into two phases, namely, a fast-initial phase and slow-secondary phase. The results are consistent with those reported by Drouiche et al. (2009) and Bazrafshan et al. (2012). According to the diagram provided for distribution of hydrolysis products at different times (Fig. S2), the highest Al_b content was at 10 min; thus, such high efficiency at 10 min can be attributed to the high content of Al_{13} polymer.

3.3.3. Effect of electrical conductivity (EC_0)

The removal efficiency rises by changing the factor from its low level to high level when the effect of an independent variable is toward the positive region. However, the negative impact causes a decrease in the removal efficiency when a factor is varied from its low level to high level (Saleh and Danmaliki, 2016; Saleh et al., 2017, 2018). In the linear regression model presented in Eq. (6), the electrical conductivity was inversely proportional to HA removal, so that the removal rate was reduced with increased electrical conductivity. As also shown in Fig. 3, in HA removal, initial concentration (C_0), initial pH (pH_0), process time (t), and pulse time (T_{pls}) have positive effects, while the electrical conductivity (EC_0) has a negative effect. The slope of the effect demonstrates the sign of the main effect (Saleh et al., 2017, 2018). This main effect plot indicates the mean response values of a variable at different levels and expresses the relative strength of each variable considered in the analysis (Adio et al., 2017). For instance, the removal of HA increased by increasing the initial concentration (C_0) between 10 and 50 mg/L. Moreover, the increase in the removal of HA by increasing the initial pH (pH_0) (from 3 to 7), process time (t) (from 10 to 70 min), and pulse time (T_{pls}), and pulse time (T_{pls}) (from 1 to 10 min), although the increase is not as significant as that in the case of initial concentration (C_0). On the other hand, there is a gradual decrease in the removal of HA by increasing the electrical conductivity (EC_0) from 500 to 2000 μS/cm.

The decrease in the removal of HA by increasing the electrical conductivity (EC_0) is likely because in the presence of potassium salt (KNO_3), due to the competitive role of ions in electrocoagulation processes, the efficiency of aluminum oxidation and hydrogen reduction is reduced since a part of the current density is consumed for nitrate reduction (Ricordel et al., 2010). Electrical conductivity, by altering solution conductivity, can also cause changes in the amount of the current passing through the system. Current density (CD) is an important factor that controls electrochemical reactions and determines coagulant dose. In the present discussion on pH and process time, it was shown that the main species responsible for coagulation in this process is Al_b or Al_{13} polymer.

In a study on the distribution of aluminum species in EC processes, Hu et al. (2016) showed that the amount of Al_b produced in electrocoagulation has an inverse relationship with the applied current density, so that a low current density results in formation of more Al_b polymer, or Al_{13}, which confirms the results of the present study (Fig. S3). They found that although an increase in current density would lead to reduced time required to reach the maximum Al_b content, the time required to reach the maximum content at a density of 10, 50, and 100 A/m^2 is approximately 5, 8, and 10 min. With increased current density, the solution pH is increased due to the increased production of OH^- in cathode, and with increased solution pH, the pure positive charge and, as a result, the repulsive force between Al_{13} polymers (the main species in the production of $Al(OH)_3$ deposits) are reduced. This facilitates accumulation of the polymers to form $Al(OH)_3$ deposits (Hu et al., 2016) (Fig. S1), but such an increase in pH would also result in the increased negative charge of HA (due to the exit of functional groups) and increased zeta potential of HA. On this basis, a low current density can be considered optimal. In a study conducted by Vasudevan et al. (2011), the best removal efficiency of cadmium was at a density of 20 A/m^2, which is close to the optimal current density of 24.3 A/m^2 in the present study. In another study conducted by Chafi et al. (2011), increasing the density up to 20 mA/cm^2 increased the removal rate, but beyond this value, increasing the current density resulted in a reduced removal rate.

3.3.4. Effect of initial HA concentration (C_0)

In the diagram presented in Fig. 3a, increasing the initial concentration led to increased removal of HA mass (mg). In the comparative experiments 18, 19, 24, and 26, it was observed that at high concentrations, the process with 10–20 min delayed pulse current reached efficiency equal to that of the DC process. Due to the off time (t_{off}) in the pulse current, a lower amount of coagulant is produced, and more time is needed to provide the required coagulant.

3.3.5. Effect of pulse time (T_{pls})

The electric dual layer structure acts as a capacitor (with certain capacity) and is charged at the beginning of the experiment and discharged at the end of the electrolysis. In the electrolysis study with DC, charging and discharging of the electrical dual layer occurs at the beginning and end of the electrolysis; however, in pulse electrolysis, due to the time gap, the charge and discharge of the electrical dual layer occurs at the beginning and end of each pulse alternating at certain time intervals (based on T_{pls}). Thus, the ratio of layer charging time to t_{on} and ratio of layer discharging t_{off} are of great importance in pulse electrolysis. The pulse electrolysis theories emphasize that the current establishment time should be so long that the electrical dual layer has enough time for charging; the off-time should be long enough for the electrical dual layer to be completely discharged. In other words, only a part of t_{on} and t_{off} is spent for charging and discharging of the electrical dual layer (Puippe and Leaman, 1986). According to the Taguchi analysis diagram presented in Fig. 3a, an increase in the pulse time led to

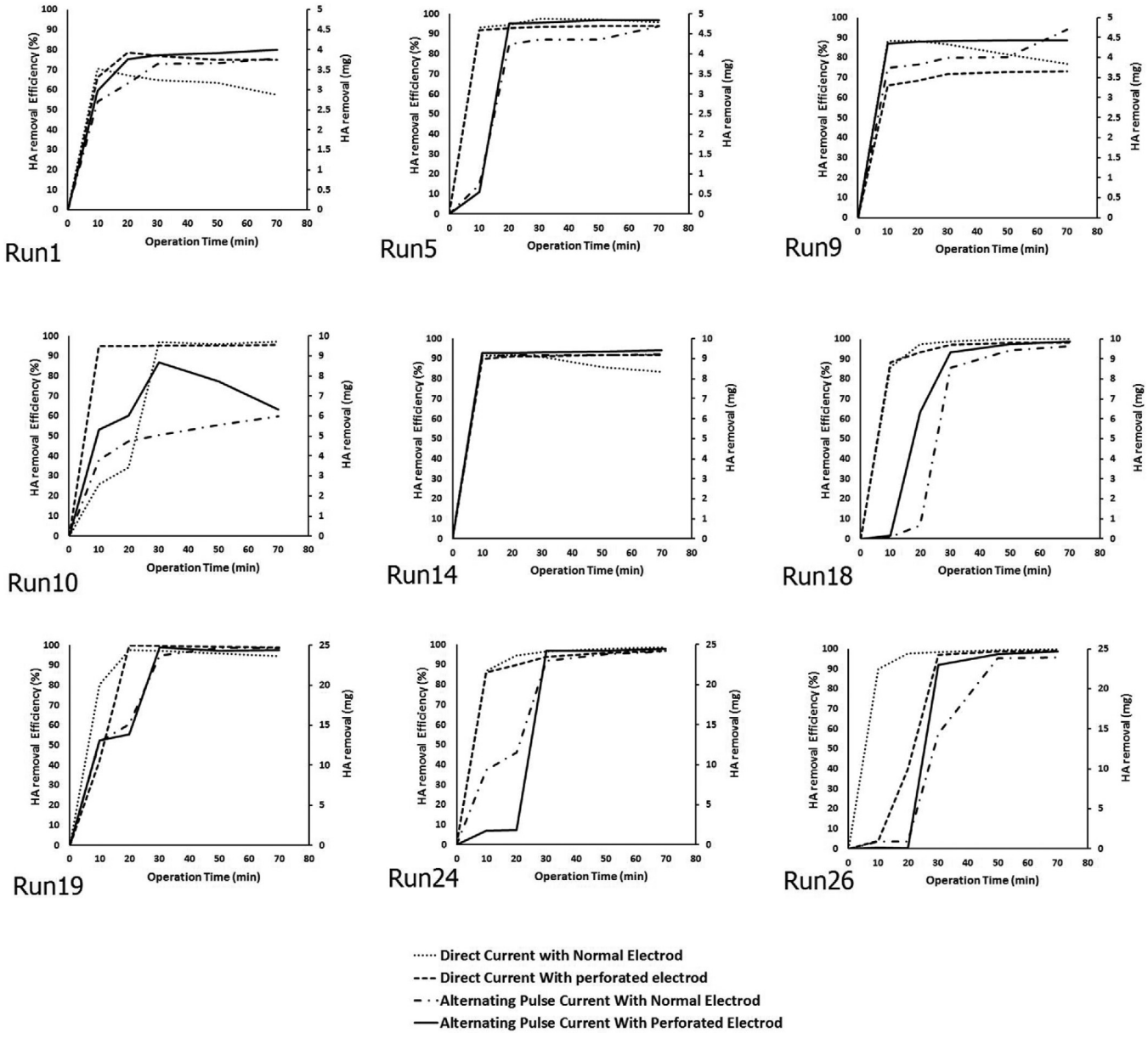

Fig. 4. Diagrams for HA removal versus process time of selected experiments (C_0 = 10–50 mg/L, pH_0 = 3–9, EC_0 = 500–2000 μS/cm, T_{pls} = 1–10 min, N_{pls} = 1–10, and V = 5–15 V) to compare four processes of DC-simple electrode, direct current-perforated electrode, pulse current-simple electrode, and pulse current-perforated electrode.

an increased removal rate. The above-mentioned data confirm the results obtained in this study.

3.4. Comparative experiments to evaluate the effect of current type and electrode shape

To investigate the effect of current type (direct and pulse) and electrode shape (perforated and simple), 9 experiments were selected from among 27 experiments covering all levels of variables (Table S3). To make a comparative analysis in terms of HA removal efficiency, the selected experiments were evaluated for four different processes including: (i) DC-simple electrode, (ii) DC-perforated electrode, (iii) pulse current-simple electrode, and (iv) pulse current-perforated electrode, the results of which are presented in Fig. 4.

In the experiment (1), in which all variables were at their lowest level, the maximum removal rate occurred in the pulse current-perforated electrode process. The process of DC with simple electrodes had the highest removal efficiency in the first 10 min, but afterwards, the removal efficiency was reduced to nearly 58%. The two processes, using perforated electrodes, exhibited better efficiency in both current states (modes).

According to the experiment (5), it is obvious that processes with pulse current (simple and perforated electrode) reached an efficiency equal to that of the process with DC after a 10-min delay. In the process with pulse current and perforated electrodes, a better efficiency was achieved compared to the pulse current and simple electrodes. In the experiment (9), compared to the experiment (5), the electrical conductivity, pulse number, and pulse time were doubled; voltage and pH were increased from 10 to 15 and from 7 to 9, respectively. After 20 min, in the process with DC and a simple electrode, the removal efficiency was reduced to nearly 78%. Due to the high voltage and electrical conductivity, there was a probability to produce excessive coagulant and re-stabilization. In the experiment (10), the main process (pulse current and perforated electrode) exhibited no acceptable efficiency compared to

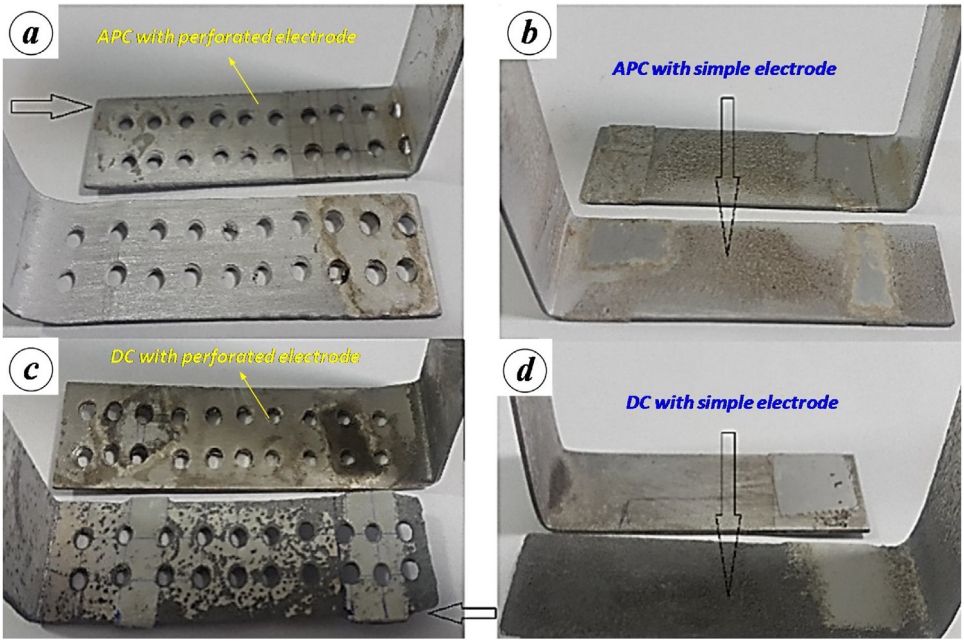

Fig. 5. Surface of electrodes in (a) pulse current with perforated electrode; (b) pulse current with simple electrode (c) DC with perforated electrode; and (d) DC with simple electrode under conditions of C_0 = 10–50 mg/L, pH_0 = 3–9, EC_0 = 500–2000 μS/cm, T_{pls} = 1–10 min, N_{pls} = 1–10, and V = 5–15 V.

the DC, and a significant reduction in efficiency was seen at 30 min because the pulse time and pulse number were under inappropriate conditions for the process with the pulse current.

In the experiment (14), all four processes had high, similar efficiencies. In the process with DC and a simple electrode, the efficiency was reduced after 30 min, which could be because the electrical conductivity and voltage variables were highest, leading to the passage of higher current density through the circuit, production of excessive coagulant, and re-stabilization. In the experiment (18), the process with pulse current could not achieve an acceptable efficiency up to the 30 min. At 70 min, the removal efficiency was almost equal in all four processes. Here, similarly, the pulse current with a perforated electrode exhibited better efficiency than the simple electrode. In the experiment (19), due to the high concentration of HA and the need for more coagulant, the efficiency with pulse current at 20 min was lower than with the DC, and the pulse current could achieve an efficiency equal to that of the DC, with a 10-min delay at 30 min.

In the experiment (24), the process with DC achieved an efficiency of 85% at 10 min, while the process with pulse current had no significant removal rate up to the 20th min; however, at 30 min, the removal efficiency reached to that of the DC. At high concentrations, due to the need for more coagulant, the process with the DC had a higher efficiency, but at low concentrations, the process with DC resulted in re-stabilization due to the production of excessive coagulant. In the experiment (26), as in the previous conditions in the process with pulse current, the removal began at 30 min and achieved an efficiency nearly equal to the DC at 70 min.

3.5. Comparing electrode surfaces in the four processes

To investigate the effect of current type (alternating pulse and DCs) and electrode's shape (simple and perforated) on the corrosion of the electrode surfaces after the end of nine comparative experiments; the used electrodes were washed with distilled water and then compared. In addition, an unused electrode was also considered as the control electrode. The electrodes used in the comparative experiments for four different processes are illustrated in Fig. 5. In Fig. 5a and b, the electrodes used in the APC, and in Fig. 5c and d, the electrodes used in the DC are shown for the two shapes of perforated and simple electrodes, respectively. As shown in Fig. 5 for the electrode surfaces, in the electrode used in the reactor with pulse current, no oxide layer formed on the electrode surface, and both electrodes were corroded equally due to changes in electrode polarity. In the electrode with DC, the corrosion rate is clearly visible, and the passive layer formed on the electrode is completely clear. The off-current time in pulse current led to formation of aluminum oxide, which was due to the O_2 species reaching distances far from the electrode surface and, as a result, lower probability of being combined with Al^{3+}; therefore, dissolution of the oxide layer and reduced probability of formation of this layer at t_{off} would lead to the formation of a thinner coating than the DC (Sahay and Kushwaha, 2017).

Passivation of aluminum electrodes is a common problem in electrocoagulation reactors in water treatment, which adds additional voltage on the system. The electrodes used in the four processes were compared in terms of their surface corrosion rate. Under a microscopic examination, the electrode surface morphology was investigated in Fig. 6 using scanning electron microscopy (SEM) at a scale of 2 μm and 500 nm. Comparing the electrode SEM images led to the conclusion that in the process with pulse current and perforated electrode, less disordered (irregular) pores were formed; an ordered structure of aluminum could be still seen, and the aluminum electrodes were dissolved uniformly. However, electrodes fed with DC had numerous nesting pores, and the accumulation of fine crystals indicated the formation of aluminum oxide. These results are consistent with those of Mao et al. (2008). Furthermore, these images also indicated that perforation of the electrodes, compared to simple electrodes, resulted in relatively more ordered pores on the electrode surface.

3.6. Investigating the concentration gradient

Fig. S4 illustrates an example of an ongoing ECF process with DC and a perforated electrode (a) and pulse current and a simple electrode (b). The two experiments were performed under the same operational conditions including C_0 = 50 mg/L, pH_0 = 9, EC_0 = 500 μS/cm, voltage = 10 V, and process time of t = 50 min. As seen

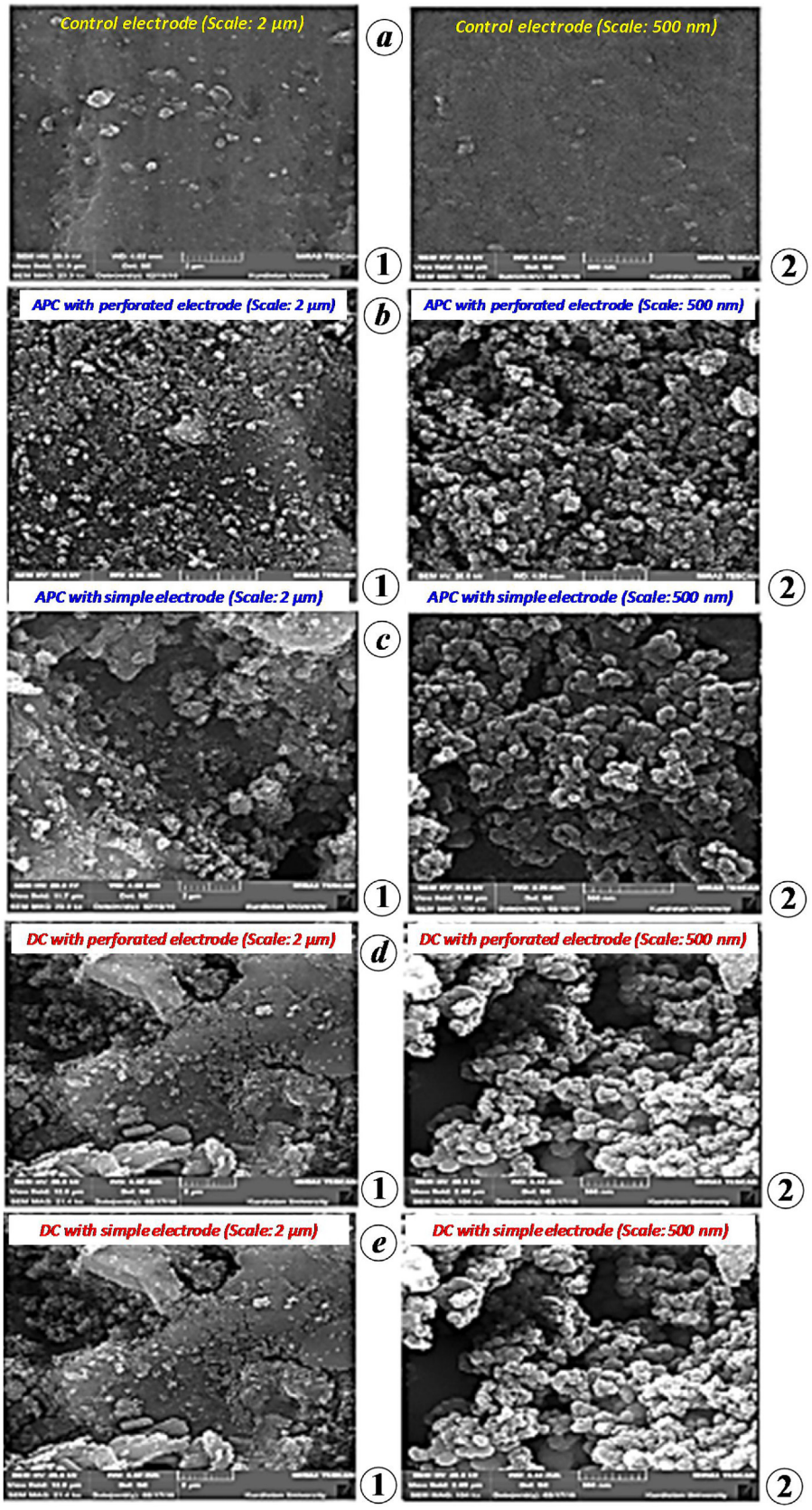

Fig. 6. Scanning electron microscopy (SEM) of (a) surface of control electrode; (b) electrode used in process with pulse current and perforated electrode; (c) electrode used in process with pulse current and simple electrode; (d) electrode used in process with DC and perforated electrode; and (e) electrode used in process with DC and simple electrode on scale of (1) 2 µm and (2) 500 nm.

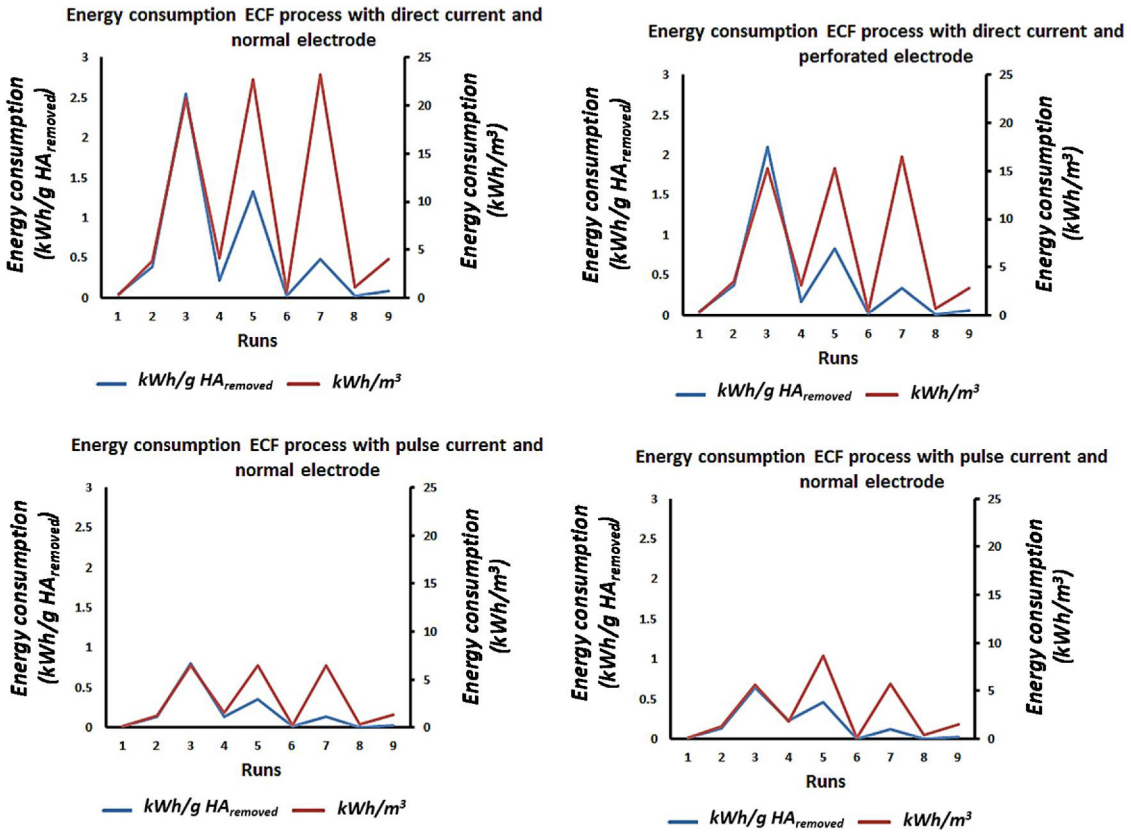

Fig. 7. Comparing energy consumption in four processes (C_0 = 10–50 mg/L, pH_0 = 3–9, EC_0 = 500–2000 μS/cm, T_{pls} = 1–10 min, N_{pls} = 1–10, and V = 5–15 V).

in section (a) of this figure, with DC, due to the created concentration gradient, no gelatin layer has formed. According to Yildiz et al. (2008), such layer is formed at high pH values and concentrations above 120 mg/L, but quite a thin layer of HA has been formed on the electrode's surface. On the other hand, in section (b), which was performed under the same operational conditions, there was no formation of a thin layer or accumulation of sludge around the electrodes.

3.7. Comparing sludge amounts and re-stabilization of processes

As seen in Fig. S5a, the amount of sludge produced in the process with a pulse current is considerably less than the process with DC under equal conditions, which is consistent with Keshmirizadeh et al. (2011), who conducted studies on chromium removal using an APC system. Fig. S5b shows an example of re-stabilization during the electrolysis with DC with a simple electrode. It was compared to the pulse current electrolysis with a perforated electrode under the operational conditions of the experiment (9) (C_0 of 10 mg/L, EC_0 of 2000 μS/cm, pH_0 of 9, voltage of 15 V, N_{pls} of 10, and T_{pls} of 10 min). Some of experiments exhibited reduced efficiency, which could be due to the excessive production of coagulant and re-stabilization of the process.

3.8. Comparing energy consumption in the four comparative processes

Fig. 7 shows the energy consumption in kWh/m^3 and kWh/g $HA_{removed}$ in the four comparative processes for each experiment. As seen from the schematics, there was a huge difference between the direct and pulse currents in terms of energy consumption. The average energy consumption for the removed HA (kWh/g $HA_{removed}$) and average efficiency (%) in nine experiments were 0.57 and 90% in the process with DC and a simple electrode, 0.43 and 91% in the process with DC and a perforated electrode, 0.17 and 85% in the process with pulse current and a simple electrode, and 0.18 and 87% in the process with pulse current and a perforated electrode, respectively. Hence, the process with alternating pulse current, with a third of the DC's energy consumption, reached an efficiency close to that with DC.

Fig. 8a represents a comparison of energy consumption (kWh/g $HA_{removed}$) and efficiency of processes (%) under operational conditions of experiment (14) (C_0 of 20 mg/L, EC_0 of 2000 μS/cm, pH_0 of 7, voltage of 15 V, N_{pls} of 10, T_{pls} of 5 min, and process time of t = 50 min), which was performed with common concentrations and pH. As indicated by the diagram, the highest efficiency (93.5%) and lowest energy consumption (0.46) were obtained with pulse current. The next highest efficiency was in the process with pulse current and a simple electrode. This was followed by DC with a perforated electrode and DC with a simple electrode resulted in the lowest efficiency (85.8%) and highest energy consumption (1.32) (conventional process), respectively.

Fig. 8b shows that, in the comparative experiments, the lowest energy consumption (kwh/$g_{removal\ HA}$) in all four processes occurred in the experimental conditions (C_0 of 50 mg/L, EC_0 of 1000 μS/cm, pH of 7, voltage of 5 V, and process time of t = 50 min). Although the process with a pulse current has a 1% lower efficiency (97%) compared to the DC (98%), the energy consumption rate in the process with pulse current (0.007 kW h/g $HA_{removed}$) was a third of the energy consumption in the process with DC (0.022 kW h/g $HA_{removed}$). According to Mao et al. (2008), the pulse current would lead to a significant reduction in energy consumption. The energy consumption rate (kWh/m^3) was equal to 1.08 for a DC with a simple electrode, 0.75 in DC with a perforated electrode, 0.38 in APC with a simple electrode, and 0.37 in pulse current with a perforated electrode.

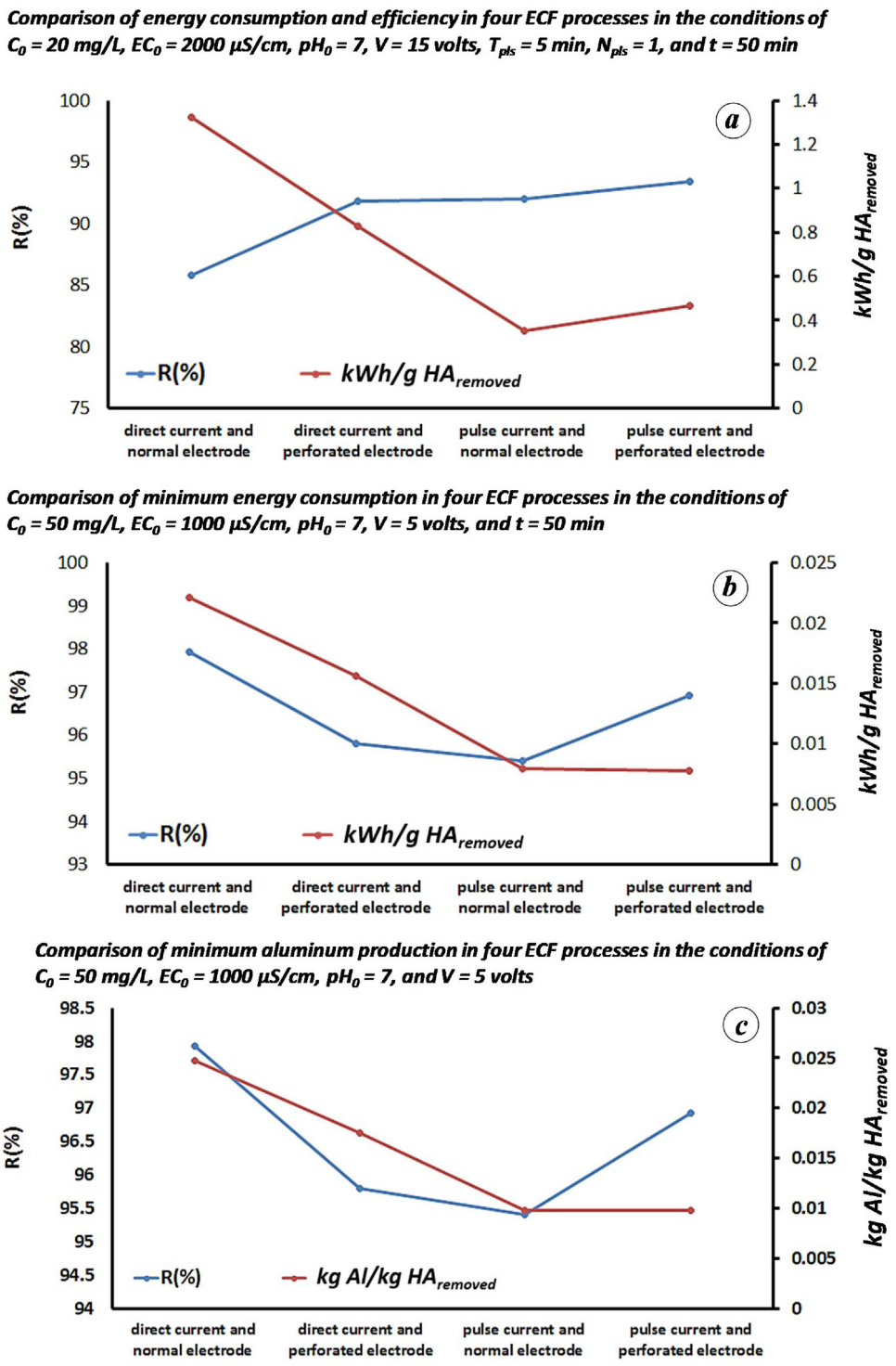

Fig. 8. (a) Energy consumption and efficiency of comparative processes; (b) minimum energy consumption rate and efficiency in comparative processes; and (c) comparing aluminum production rate.

It is noted that pulse current leads to less energy consumption and coagulant production, which in turn causes less efficiency. Also, perforated electrodes lead to the same impact by reducing surface area of electrodes. Therefore, it is expected that their combination causes less energy consumption and efficiency, but the results shows the consistent energy consumption and improvement in efficiency. This is risen from the complex nature of electrocoagulation. The pulse current leads to less concentration polarization that in turn leads to more coagulation and more efficiency. Additionally, the perforating of electrodes leads to increase in sharp edges on electrodes that are more electro-active area because of more current density. This effect is well known in corrosion science. In this regard, results of the present study show a synergistic effect that leads to increase in efficiency by applying both pulse current and perforated electrodes simultaneously.

In another study, Yildiz et al. (2008) achieved an efficiency of 81.2% at an initial HA concentration of 200 without adding electrolyte at a pH of 7, a time of 55 min and with an energy

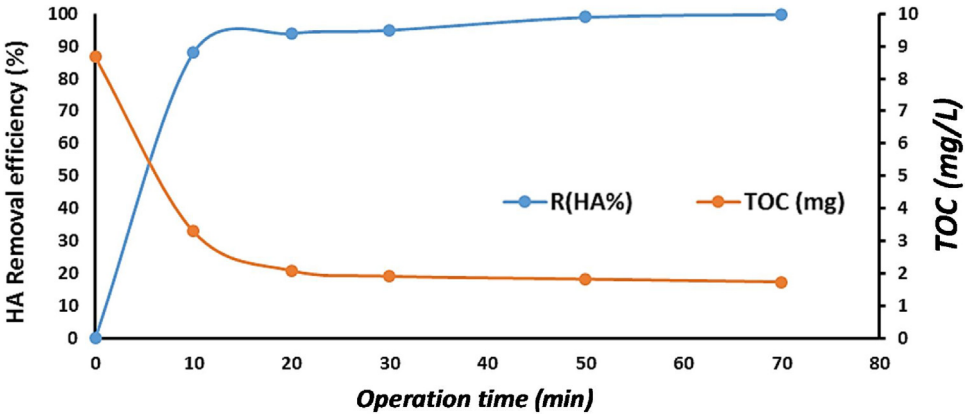

Fig. 9. Diagram for removal of HA and TOC under the optimal conditions (pH_0 of 6.6, CD of 24.3 A/m^2, T_{pls} of 10 min, N_{puls} of 3, EC_0 of 800 μS/cm, and C_0 of 20 mg/L).

consumption rate of 3.18 kW h/m^3 with a DC. Furthermore, in the present study, an efficiency of 81.2% was obtained at the solution's pH and at concentration of 200 (pH of 9), process time of 60 min, and energy consumption rate of 2 kW h/m^3. In a study conducted by Vasudevan et al. (2011), the best cadmium removal efficiency using an aluminum anode and cathode at a current density of 20 A/m^2 and pH of 7 was obtained at 97.5% for an alternating current with an energy consumption rate of 0.454 kW h/m^3 and 96.2% for a DC with an energy consumption rate of 1.002 kW h/m^3. The energy consumption ratio in two currents was equal to 2.2, which is close to that obtained in the present study (i.e., 3).

3.9. Comparing aluminum consumption rate

The average aluminum consumption for removed HA (kg Al/kg $HA_{removed}$) in nine experiments was 0.236 in the process with a DC and a simple electrode, 0.182 in the process with a DC and a perforated electrode, 0.089 in the process with a pulse current and a simple electrode, and 0.09 in the process with a pulse current and a perforated electrode. According to the diagram in Fig. 8c in the comparative experiments, the minimum aluminum consumption rate (kg Al/kg $HA_{removed}$) in all four processes was obtained at conditions of C_0 = 50 mg/L, EC_0 = 1000 μS/cm, pH_0 = 7, and V = 5 V. Although the process with a pulse current had a 1% lower efficiency (97%) compared to the DC (98%), the aluminum consumption rate in DC (0.024) was twice that in the process with pulse current (0.01), which would lead to reduced process costs and a lower energy consumption rate.

Finally, a further experiment was performed at a HA concentration common in surface waters and under the obtained optimal conditions based on linear regression and artificial neural network modeling (pH_0 of 6.6, CD of 24.3 A/m^2, T_{pls} of 10 min, N_{puls} of 3, EC_0 of 800 μS/cm, and C_0 of 20 mg/L). The results were measured using a spectrophotometer and a TOC-meter device. These results are shown in Fig. 9. The British standard for all THMs is 100 μg/L, while the THMs formation potential by natural substances is more than 100 μg for each 1 mg of dissolved organic carbon (DOC). If 1 mg/L of DOC remains, it can increase the trihalomethane concentration to 100 μg/L, and thus break the above-mentioned standard (Edzwald and Tobiason, 1999; Murray and Parsons, 2006; US EPA, 2006). The measurements showed an initial DOC content and residual DOC of 8.67 and 1.7 mg/L, respectively. Thus, according to the above explanations, it cannot meet the given standard, so that additional treatment might be required.

4. Conclusions

A six factor (initial concentration, initial pH, electrical conductivity, pulse time, pulse number, and process time), three-level, L27 orthogonal array of Taguchi/DOE-based optimization were implemented as an effective tool for mathematical modeling of HA removal for the comparative analysis of four different ECF processes. Based on both experimental and modeling results, conclusions drawn from the present study and final remarks are summarized as follows:

(1) According to the results obtained from multiple linear regression, the independent variables, including initial concentration, pH, process time, and pulse time were directly, but electrical conductivity was inversely proportional to the HA removal rate.
(2) APC-ECF method led to the production of less dewatered and dense sludge, and the morphology of the electrode surfaces with APC and perforated electrode showed less disordered (irregular) pores and a regular structure of aluminum compared to the DC.
(3) In the comparative experiments, the average energy consumption (kWh/g $HA_{removed}$) and average removal efficiency (%) in nine experiments were equal to 0.57 and 90% in the process with a DC and a simple electrode and 0.18 and 87% in the process with an APC and a perforated electrode.
(4) The APC process, with one-third of the energy consumption of DC, reached a similar efficiency close to that of DC. Furthermore, the average aluminum consumption for removed HA (kg Al/g $HA_{removed}$) in nine experiments in the process with a DC and a simple electrode was 2.5-fold higher (0.236) than that obtained in the process with a pulse current and perforated electrode (0.09).
(5) In addition to numerous advantages, such as the prevention of the formation of an oxide layer on the electrode surface, lower electrode consumption, dewatered and dense sludge production (which is of great importance in sludge disposal costs), electrocoagulation with APC can also achieve an efficiency close to that of a DC process but at one-third of the energy consumption rate. Since power consumption costs account for more than 50% of the expenses of the electrocoagulation unit, it is highly important to improve the electrolytic processes for electrocoagulation application.
(6) The ECF process can be used for a wide range of water and wastewater treatment systems that are highly effective in removal of mineral contaminants and pathogens. Due to the extensive application of this process, it can be used for the treatment of surface and underground water.

Conflict of interest

The authors declare that they have no conflict of interest.

Acknowledgements

This study was based on the Research Dissertation work of the first author and approved by the Environmental Health Research Center and funded by the Kurdistan University of Medical Sciences. The authors extend their special thanks to the sponsors of the project.

Appendix A. Supplementary data

Supplementary material related to this article can be found, in the online version, at doi:https://doi.org/10.1016/j.psep.2018.10.025.

References

Adio, S.O., Omar, M.H., Asif, M., Saleh, T.A., 2017. Arsenic and selenium removal from water using biosynthesized nanoscale zero-valent iron: a factorial design analysis. Process Saf. Environ. Prot. 107, 518–527, http://dx.doi.org/10.1016/j.psep.2017.03.004.

Alimohammadi, M., Askari, M., Dehghani, M.H., Dalvand, A., Saeedi, R., Yetilmezsoy, K., Heibati, B., McKay, G., 2017. Elimination of natural organic matter by electrocoagulation using bipolar and monopolar arrangements of iron and aluminum electrodes. Int. J. Environ. Sci. Technol. 14 (10), 2125–2134, http://dx.doi.org/10.1007/s13762-017-1402-3.

Alswat, A.A., Ahmad, M.B., Hussein, M.Z., Ibrahim, N.A., Saleh, T.A., 2017a. Copper oxide nanoparticles-loaded zeolite and its characteristics and antibacterial activities. J. Mater. Sci. Technol. 33 (8), 889–896, http://dx.doi.org/10.1016/j.jmst.2017.03.015.

Alswat, A.A., Ahmad, M.B., Saleh, T.A., 2017b. Preparation and characterization of zeolitezinc oxide-copper oxide nanocomposite: antibacterial activities. Colloid. Interface Sci. Commun. 16, 19–24, http://dx.doi.org/10.1016/j.colcom.2016.12.003.

Bajpai, J., Bajpai, A.K., Chhatri, A., Lawrance, S., Dsouza, A., 2014. A critical review on the state-of-art of water pollution by heavy metals and fluoride ions and defluoridation techniques. Chem. Sci. Rev. Lett. 3 (11S), 210–223.

Bazrafshan, E., Mahvi, A.H., Nasseri, S., Shaieghi, M., 2007. Performance evaluation of electrocoagulation process for diazinon removal from aqueous environments by using iron electrodes. J. Environ. Health Sci. Eng. 4 (2), 127–132.

Bazrafshan, E., Biglari, H., Mahvi, A.H., 2012. Humic acid removal from aqueous environments by electrocoagulation process using iron electrodes. J. Chem. 9 (4), 2453–2461, http://dx.doi.org/10.1155/2012/876739.

Chafi, M., Gourich, B., Essadki, A.H., Vial, C., Fabregat, A., 2011. Comparison of electrocoagulation using iron and aluminium electrodes with chemical coagulation for the removal of a highly soluble acid dye. Desalination 281, 285–292, http://dx.doi.org/10.1016/j.desal.2011.08.004.

Crittenden, J.C., Montgomery-Watson, H., 2005. Water Treatment Principles and Design. John Wiley & Sons, Hoboken, NJ, USA.

Daneshvar, N., Khataee, A.R., Rasoulifard, M.H., Pourhassan, M., 2007. Biodegradation of dye solution containing Malachite Green: optimization of effective parameters using Taguchi method. J. Hazard. Mater. 143 (1), 214–219, http://dx.doi.org/10.1016/j.jhazmat.2006.09.016.

De la Rubia, M.Á., Rodríguez, M., Prats, D., 2006. pH, ionic strength and flow velocity effects on the NOM filtration with TiO/ZrO membranes. Sep. Purif. Technol. 52 (2), 325–331, http://dx.doi.org/10.1016/j.seppur.2006.05.007.

Drouiche, N., Aoudj, S., Hecini, M., Ghaffour, N., Lounici, H., Mameri, N., 2009. Study on the treatment of photovoltaic wastewater using electrocoagulation: fluoride removal with aluminium electrodes. J. Hazard. Mater. 169 (1), 65–69, http://dx.doi.org/10.1016/j.jhazmat.2009.03.073.

Edzwald, J.K., Tobiason, J.E., 1999. Enhanced coagulation: US requirements and a broader view. Water Sci. Technol. 40 (9), 63–70, http://dx.doi.org/10.1016/S0273-1223(99)00641-1.

Eish, M.Y.Z.A., Wells, M.J.M., 2006. Assessing the trihalomethane formation potential of aquatic fulvic and humic acids fractionated using thin-layer chromatography. J. Chromatogr. A 1116 (1), 272–276, http://dx.doi.org/10.1016/j.chroma.2006.03.064.

El khalidi, Z., Hartiti, B., Fadili, S., Thevenin, P., 2018. Nickel oxide optimization using Taguchi design for hydrogen detection. Int. J. Hydrogen Energy 43, 12574–12583, http://dx.doi.org/10.1016/j.ijhydene.2018.04.162.

Feng, Q.-y., Li, X.-d., Cheng, Y.-j., Meng, L., Meng, Q.-j., 2007. Removal of humic acid from groundwater by electrocoagulation. J. China Univ. Mining. Technol. 17 (4), 513–520, http://dx.doi.org/10.1016/S1006-1266(07)60136-9.

Gregor, J.E., Nokes, C.J., Fenton, E., 1997. Optimising natural organic matter removal from low turbidity waters by controlled pH adjustment of aluminium coagulation. Water Res. 31 (12), 2949–2958, http://dx.doi.org/10.1016/S0043-1354(97)00154-1.

Hasani, G., Daraei, H., Shahmoradi, B., Gharibi, F., Maleki, A., Yetilmezsoy, K., McKay, G., 2018. A novel ANN approach for modeling of alternating pulse current electrocoagulation-flotation (APC-ECF) process: humic acid removal from aqueous media. Process Saf. Environ. Prot. 117, 111–124, http://dx.doi.org/10.1016/j.psep.2018.04.017.

Holt, P.K., Barton, G.W., Wark, M., Mitchell, C.A., 2002. A quantitative comparison between chemical dosing and electrocoagulation. Colloids Surf. A Physicochem. Eng. Asp. 211 (2), 233–248, http://dx.doi.org/10.1016/S0927-7757(02)00285-6.

Hu, C., Wang, S., Sun, J., Liu, H., Qu, J., 2016. An effective method for improving electrocoagulation process: optimization of Al_{13} polymer formation. Colloids Surf. A Physicochem. Eng. Asp. 489, 234–240, http://dx.doi.org/10.1016/j.colsurfa.2015.10.063.

Jafari, A., Mahvi, A.H., Nasseri, S., Rashidi, A., Nabizadeh, R., Rezaee, R., 2015. Ultrafiltration of natural organic matter from water by vertically aligned carbon nanotube membrane. J. Environ. Health Sci. Eng. 13 (51), 1–9, http://dx.doi.org/10.1186/s40201-015-0207-x.

Kawamura, S., 2000. Integrated Design and Operation of Water Treatment Facilities. John Wiley & Sons, NY, USA.

Keshmirizadeh, E., Yousefi, S., Rofouei, M.K., 2011. An investigation on the new operational parameter effective in Cr (VI) removal efficiency: a study on electrocoagulation by alternating pulse current. J. Hazard. Mater. 190 (1), 119–124, http://dx.doi.org/10.1016/j.jhazmat.2011.03.010.

Koparal, A.S., Yildiz, Y.S., Keskinler, B., Demircioglu, N., 2008. Effect of initial pH on the removal of humic substances from wastewater by electrocoagulation. Sep. Purif. Technol. 59 (2), 175–182, http://dx.doi.org/10.1016/j.seppur.2007.06.004.

Li, A., Zhao, X., Liu, H., Qu, J., 2011. Characteristic transformation of humic acid during photoelectrocatalysis process and its subsequent disinfection byproduct formation potential. Water Res. 45 (18), 6131–6140, http://dx.doi.org/10.1016/j.watres.2011.09.012.

Lu, X., Chen, Z., Yang, X., 1999. Spectroscopic study of aluminium speciation in removing humic substances by Al coagulation. Water Res. 33 (15), 3271–3280, http://dx.doi.org/10.1016/S0043-1354(99)00047-0.

Mahvi, A.H., Maleki, A., Rezaee, R., Safari, M., 2009. Reduction of humic substances in water by application of ultrasound waves and ultraviolet irradiation. J. Environ. Health Sci. Eng. 6 (4), 233–240.

Malakootian, M., Yousefi, N., Fatehizadeh, A., 2011. Survey efficiency of electrocoagulation on nitrate removal from aqueous solution. Int. J. Environ. Sci. Technol. 8 (1), 107–114, http://dx.doi.org/10.1007/BF03326200.

Maleki, A., Safari, M., Shahmoradi, B., Zandsalimi, Y., Daraei, H., Gharibi, F., 2016a. Photocatalytic degradation of humic substances in aqueous solution using Cu-doped ZnO nanoparticles under natural sunlight irradiation. Environ. Sci. Pollut. Res. 22 (21), 16875–16880, http://dx.doi.org/10.1007/s11356-015-4915-7.

Maleki, A., Safari, M., Rezaee, R., Cheshmeh Soltani, R.D., Shahmoradi, B., Zandsalimi, Y., 2016b. Photocatalytic degradation of humic substances in the presence of ZnO nanoparticles immobilized on glass plates under ultraviolet irradiation. Sep. Sci. Technol. 51 (14), 2484–2489, http://dx.doi.org/10.1080/01496395.2016.1213746.

Mao, X., Hong, S., Zhu, H., Lin, H., Wei, L., Gan, F., 2008. Alternating pulse current in electrocoagulation for wastewater treatment to prevent the passivation of al electrode. J. Wuhan Univ. Technol.-Mater. Sci. Ed. 23 (2), 239–241, http://dx.doi.org/10.1007/s11595-006-2239-7.

Martinez-Huitle, C.A., Brillas, E., 2009. Decontamination of wastewaters containing synthetic organic dyes by electrochemical methods: a general review. Appl. Catal B-Environ. 87 (3), 105–145, http://dx.doi.org/10.1016/j.apcatb.2008.09.017.

Mohora, E., Rončević, S., Agbaba, J., Tubić, A., Mitić, M., Klašnja, M., Dalmacija, B., 2014. Removal of arsenic from groundwater rich in natural organic matter (NOM) by continuous electrocoagulation/flocculation (ECF). Sep. Purif. Technol. 136, 150–156, http://dx.doi.org/10.1016/j.seppur.2014.09.006.

Mollah, M.Y.A., Schennach, R., Parga, J.R., Cocke, D.L., 2001. Electrocoagulation (EC) – science and applications. J. Hazard. Mater. 84 (1), 29–41, http://dx.doi.org/10.1016/S0304-3894(01)00176-5.

Moura, M.N., Martín, M.J., Burguillo, F.J., 2007. A comparative study of the adsorption of humic acid, fulvic acid and phenol onto *Bacillus subtilis* and activated sludge. J. Hazard. Mater. 149 (1), 42–48, http://dx.doi.org/10.1016/j.jhazmat.2007.02.074.

Murray, C.A., Parsons, S.A., 2006. Preliminary laboratory investigation of disinfection by-product precursor removal using an advanced oxidation process. Water Environ. J. 20 (3), 123–129, http://dx.doi.org/10.1111/j.1747-6593.2005.00004.x.

Oztop, M.H., Sahin, S., Sumnu, G., 2007. Optimization of microwave frying of potato slices by using Taguchi technique. J. Food Eng. 79 (1), 83–91, http://dx.doi.org/10.1016/j.jfoodeng.2006.01.031.

Puippe, J.C., Leaman, F., 1986. Theory and Practice of Pulse Plating. American Electroplaters and Surface Finishers Society.

Rao, G., Zhang, Q., Zhao, H., Chen, J., Li, Y., 2016. Novel titanium dioxide/iron (III) oxide/graphene oxide photocatalytic membrane for enhanced humic acid removal from water. Chem. Eng. J. 302, 633–640, http://dx.doi.org/10.1016/j.cej.2016.05.095.

Rauthula, M.S., Srivastava, V.C., 2011. Studies on adsorption/desorption of nitrobenzene and humic acid onto/from activated carbon. Chem. Eng. J. 168 (1), 35–43, http://dx.doi.org/10.1016/j.cej.2010.12.026.

Ricordel, C., Darchen, A., Hadjiev, D., 2010. Electrocoagulation/electroflotation as a surface water treatment for industrial uses. Sep. Purif. Technol. 74 (3), 342–347, http://dx.doi.org/10.1016/j.seppur.2010.06.024.

Rodriguez, M.J., Serodes, J.-B., Levallois, P., 2004. Behavior of trihalomethanes and haloacetic acids in a drinking water distribution system. Water Res. 38 (20), 4367–4382, http://dx.doi.org/10.1016/j.watres.2004.08.018.

Sachse, A., Henrion, R., Gelbrecht, J., Steinberg, C.E.W., 2005. Classification of dissolved organic carbon (DOC) in river systems: influence of catchment characteristics and autochthonous processes. Org. Geochem. 36 (6), 923–935, http://dx.doi.org/10.1016/j.orggeochem.2004.12.008.

Safari, M., Rezaee, A., Ayati, B., Jonidi-Jafari, A., 2014. Bio-electrochemical reduction of nitrate utilizing MWCNT supported on carbon base electrodes: a comparison study. J. Taiwan Inst. Chem. Eng. 45 (5), 2212–2216, http://dx.doi.org/10.1016/j.jtice.2014.05.006.

Sahay, P.P., Kushwaha, A.K., 2017. Electrochemical supercapacitive performance of potentiostatically cathodic electrodeposited nanostructured MnO_2 films. J. Solid State Electrochem. 21 (8), 2393–2405, http://dx.doi.org/10.1007/s10008-017-3574-7.

Saleh, T.A., 2015a. Mercury sorption by silica/carbon nanotubes and silica/activated carbon: a comparison study. J. Water Supply Res. Technol.-Aqua 64 (8), 892–903, http://dx.doi.org/10.2166/aqua.2015.050.

Saleh, T.A., 2015b. Isotherm, kinetic, and thermodynamic studies on Hg(II) adsorption from aqueous solution by silica-multiwall carbon nanotubes. Environ. Sci. Pollut. Res. 22 (21), 16721–16731, http://dx.doi.org/10.1007/s11356-015-4866-z.

Saleh, T.A., 2016. Nanocomposite of carbon nanotubes/silica nanoparticles and their use for adsorption of Pb(II): from surface properties to sorption mechanism. Desalin. Water Treat. 57 (23), 10730–10744, http://dx.doi.org/10.1080/19443994.2015.1036784.

Saleh, T.A., Danmaliki, G.I., 2016. Adsorptive desulfurization of dibenzothiophene from fuels by rubber tyres-derived carbons: kinetics and isotherms evaluation. Process Saf. Environ. Prot. 102, 9–19, http://dx.doi.org/10.1016/j.psep.2016.02.005.

Saleh, T.A., Sarı, A., Tuzen, M., 2017. Optimization of parameters with experimental design for the adsorption of mercury using polyethylenimine modified-activated carbon. J. Environ. Chem. Eng. 5 (1), 1079–1088, http://dx.doi.org/10.1016/j.jece.2017.01.032.

Saleh, T.A., Tuzen, M., Sarı, A., 2018. Polyamide magnetic palygorskite for the simultaneous removal of Hg(II) and methyl mercury; with factorial design analysis. J. Environ. Manage. 211, 323–333, http://dx.doi.org/10.1016/j.jenvman.2018.01.050.

Sani, H.A., Ahmad, M.B., Hussein, M.Z., Ibrahim, N.A., Musa, A., Saleh, T.A., 2017. Nanocomposite of ZnO with montmorillonite for removal of lead and copper ions from aqueous solutions. Process Saf. Environ. Prot. 109, 97–105, http://dx.doi.org/10.1016/j.psep.2017.03.024.

Seredynska-Sobecka, B., Tomaszewska, M., Morawski, A.W., 2006. Removal of humic acids by the ozonation-biofiltration process. Desalination 198 (1), 265–273, http://dx.doi.org/10.1016/j.desal.2006.01.027.

Szymański, K., Morawski, A.W., Mozia, S., 2016. Humic acids removal in a photocatalytic membrane reactor with a ceramic UF membrane. Chem. Eng. J. 305, 19–27, http://dx.doi.org/10.1016/j.cej.2015.10.024.

US EPA, 2006. Initial Distribution System Evaluation Guidance Manual. For the Final Stage 2 Disinfectants and Disinfection Byproducts Rule, EPA 815-B-06-002.

Vasudevan, S., Lakshmi, J., Sozhan, G., 2011. Effects of alternating and direct current in electrocoagulation process on the removal of cadmium from water. J. Hazard. Mater. 192 (1), 26–34, http://dx.doi.org/10.1016/j.jhazmat.2011.04.081.

Wang, C.-T., Chou, W.-L., Kuo, Y.-M., 2009. Removal of COD from laundry wastewater by electrocoagulation/electroflotation. J. Hazard. Mater. 164 (1), 81–86, http://dx.doi.org/10.1016/j.jhazmat.2008.07.122.

Wang, Y., Wang, Q., Gao, B.-Y., Yue, Q., Zhao, Y., 2012. The disinfection by-products precursors removal efficiency and the subsequent effects on chlorine decay for humic acid synthetic water treated by coagulation process and coagulation ultrafiltration process. Chem. Eng. J. 193–194 (Supplement C), 59–67, http://dx.doi.org/10.1016/j.cej.2012.04.003.

Wang, Z., Ding, J., Xie, P., Chen, Y., Wang, S., 2018. Formation of halogenated by-products during chemical cleaning of humic acid-fouled UF membrane by sodium hypochlorite solution. Chem. Eng. J. 332, 76–84, http://dx.doi.org/10.1016/j.cej.2017.09.053.

Wei, M.-C., Wang, K.-S., Hsiao, T.-E., Lin, I.-C., Wu, H.-J., Wu, Y.-L., Liu, P.-H., Chang, S.-H., 2011. Effects of UV irradiation on humic acid removal by ozonation, Fenton and Fe°/air treatment: THMFP and biotoxicity evaluation. J. Hazard. Mater. 195 (Supplement C), 324–331, http://dx.doi.org/10.1016/j.jhazmat.2011.08.044.

Yetilmezsoy, K., Ilhan, F., Sapci-Zengin, Z., Sakar, S., Gonullu, M.T., 2009a. Decolorization and COD reduction of UASB pretreated poultry manure wastewater by electrocoagulation process: a post-treatment study. J. Hazard. Mater. 162 (1), 120–132, http://dx.doi.org/10.1016/j.jhazmat.2008.05.015.

Yetilmezsoy, K., Demirel, S., Vanderbei, R.J., 2009b. Response surface modeling of Pb (II) removal from aqueous solution by *Pistacia vera* L.: Box–Behnken experimental design. J. Hazard. Mater. 171 (1–3), 551–562, http://dx.doi.org/10.1016/j.jhazmat.2009.06.035.

Yildiz, Y.S., Koparal, A.S., Keskinler, B., 2008. Effect of initial pH and supporting electrolyte on the treatment of water containing high concentration of humic substances by electrocoagulation. Chem. Eng. J. 138 (1), 63–72, http://dx.doi.org/10.1016/j.cej.2007.05.029.

Yu, W.-Z., Gregory, J., Li, G.-B., Qu, J.-H., 2013. Effect of humic acid on coagulation performance during agregation at low temperature. Chem. Eng. J. 223, 412–417, http://dx.doi.org/10.1016/j.cej.2013.03.008.

Zaleschi, L., Secula, M.S., Teodosiu, C., Stan, C.S., Cretescu, I., 2014. Removal of Rhodamine 6G from aqueous effluents by electrocoagulation in a batch reactor: assessment of Operational parameters and process mechanism. Water Air Soil Pollut. Focus. 225 (9), 2101, http://dx.doi.org/10.1007/s11270-014-2101-z.